PAPER

Interaction, bond formation or reaction between a dimethylamino group and an adjacent alkene or aldehyde group in aromatic systems controlled by remote molecular constraints†

Jonathan C. Bristow, Stacey V. A. Cliff, Songjie Yang and John D. Wallis (ID) *

Peri–peri interactions in naphthalene systems control the degree of bond formation between a *peri*-dimethylamino group and a polarised alkene or aldehyde group. Two *peri*-phenyl groups, which repel, induce closer N⋯C interactions or bond formation, while the ethylene link in the corresponding acenaphthene system has the opposite effect, and for the more electron-deficient alkenes lead to formation of a fused azepine ring initiated by the *tert*-amino effect. In related 1,8-fluorene derivatives N⋯C interactions occur for an aldehyde and a moderately polarised alkene, but fused azocines are formed when the alkene is more reactive.

Introduction

Intramolecular interactions between a nucleophile and an electrophile can be considered as representing different stages of the reaction between them, depending on their separation.[1] This approach originated with structural studies on *trans*-annular N⋯C=O interactions in pyrrolizidine alkaloids.[2] However, the *peri*-naphthalene skeleton has provided a more convenient system open to the study of a wide variety of such interactions starting with the X-ray structural determinations of Dunitz *et al.* on $Me_2N/C=O$, $MeO/C=O$ and $HO/C=O$ systems as in **1–3**.[3] Such interactions can change the chemical properties of the groups, *e.g.* the dimethylamino aldehyde **4** protonates on oxygen, not nitrogen, with HCl to give salt **5** with formation of a N–C bond.[4,5] Studies have been extended to interactions between electron-rich centres and electrophilic polar multiple bonds such as alkynes, nitriles and alkenes in **6–8**.[6–10] The interactions between a dimethylamino group and a range of polarised alkenes has been studied the most intensively. For the most electrophilic alkenes a long bond (1.60–1.66 Å) can form between the two groups producing a zwitterionic doubly fused five-membered ring *e.g.* in **9** and **10**. The constraint applied by the *peri*-naphthalene system has been used for studying other interactions such as unusual hydrogen bonding situations[11] and through space magnetic coupling between specific elements.[12] The 2,2'-disubstituted biphenyl system has also been employed, with the 1,5 interactions in naphthalenes replaced by 1,6 interactions with greater freedom of movement between the groups due to the
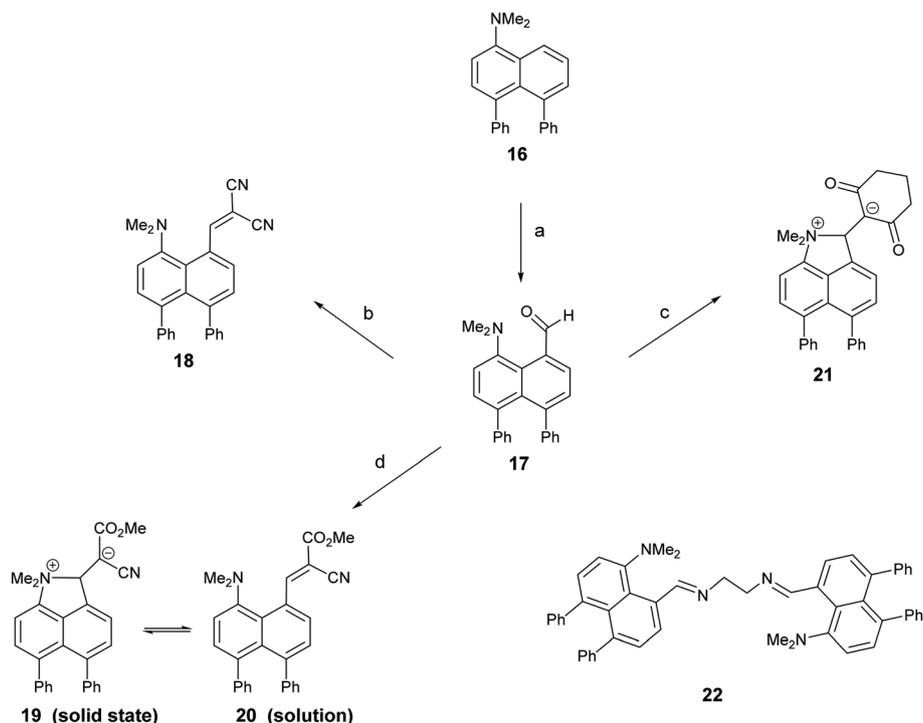
possibility of rotation about the inter–ring bond. Thus, there is a long $Me_2N⋯CHO$ interaction in **11** (2.989(2) Å), but formation of a zwitterion with a six-membered ring in **12**, with a Me_2N^+–$C(CN)_2^-$ bond (1.586(3) and 1.604(3) Å).[13]
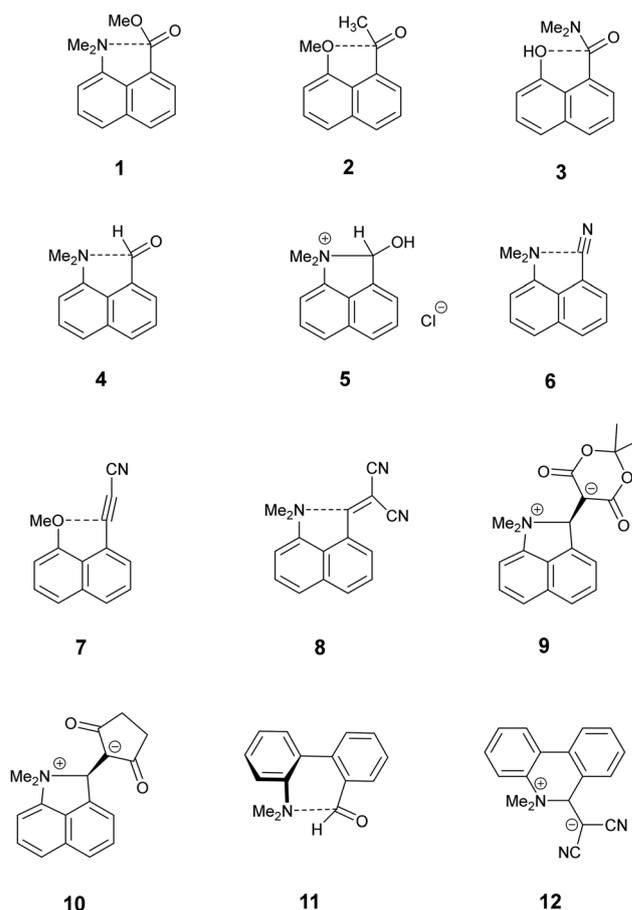
School of Science and Technology, Nottingham Trent University, Clifton Lane, Nottingham NG11 8NS, UK. E-mail: john.wallis@ntu.ac.uk

Scheme 1 (a) *n*-BuLi/hexane/80 °C/72 h; DMF/THF/−78 °C; (b)–(d) malonitrile, methyl cyanoacetate or cyclohexane-1,3-dione/ethylenediammonium diacetate cat./methanol/reflux.

Recently we demonstrated that for *peri*-naphthalenes containing a Me$_2$N- group adjacent to a –CH═C(CN)$_2$ group, the Me$_2$N···C═C separations can be controlled by substituents at the opposite pair of *peri*-positions, *e.g.* an ethylene bridge as in acenaphthene **13** opens up the separation between the two groups, while two *peri*-phenyl groups, which repel each other, reduces the separation in **14**.[14] Furthermore, we observed a temperature variable separation between the groups in the salt **15**. Remarkably the Me$_2$N···C separation at 200 K is 2.098(4) Å but reversibly contracts to 1.749(3) Å at 100 K. From all these data we were able to propose a preliminary reaction coordinate for the reaction between the groups. Here we now report the structures of two families of *peri*-naphthalenes with a dimethylamino group next to different electrophilic groups with either an ethylene bridge or two phenyl groups at the opposite *peri*-positions. Furthermore, we report the structures of a small family of 9,9-dimethylfluorenes with dimethylamino and electrophilic groups adjacent, which are designed as modified biphenyl systems in which the phenyl rings are constrained to be close to coplanar but pulled away from each other by the single carbon link between the two rings. A *peri*-disubstituted acenaphthene system has been used to investigate nucleophilic attack at silicon[15] and to prepare frustrated lone pair systems.[16]
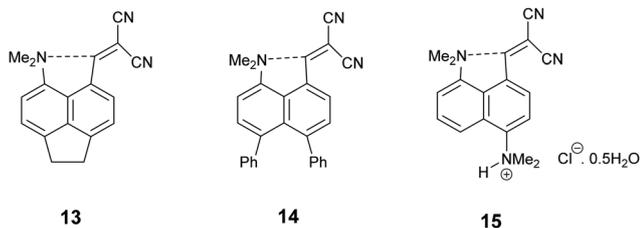
Discussion

Peri-Diphenyls derivatives

1,8-Diphenylnaphthalene[17] was converted in three steps to its 4-dimethylamino derivative **16**, which was *peri*-lithiated using *n*-butyl lithium, and converted to the aldehyde **17** with DMF in 34% yield. The aldehyde underwent Knoevenagel condensations with malonitrile, methyl cyanoacetate and cyclohexan-1,3-dione to give three derivatives **18**, **20** and **21** with two nitriles, a nitrile and an ester or a cyclic diketone, respectively, which activate the alkene to nucleophilic attack from the adjacent dimethylamino group (Scheme 1). Solution NMR studies suggests that only **21** has a bond between the *peri*-groups, since there is no low field ^{13}C NMR resonance at *ca.* 160 ppm for the *peri*-alkene carbon but a signal instead at 89.8 ppm. The crystal structures of the dimethylamino derivative **16**, the *peri*-aldehyde **17** and the Knoevenagel products were determined by X-ray crystallography to study the interaction between the functional groups. We have already reported the structure of **18**.[14]

Comparison of the structures of the dimethylamino derivative **16** and the *peri*-dimethylamino-aldehyde **17** show how the nitrogen lone pair which is partially conjugated with the naphthalene ring in **16** has oriented towards the aldehyde carbon in **17** (Fig. 1). Thus, the torsion angles of the N–CH$_3$ bonds with the aromatic ring in aldehyde **17** are much less asymmetric: 51.6(3)/−78.0(3) *cf.* 23.9(2)/−105.1(2)° in **16**, as the lone pair is rotated further away from alignment with the p orbitals of the aromatic ring (Table 1). The two phenyl rings in aldehyde **17** are tilted at 56.7 and 59.2° in the same sense
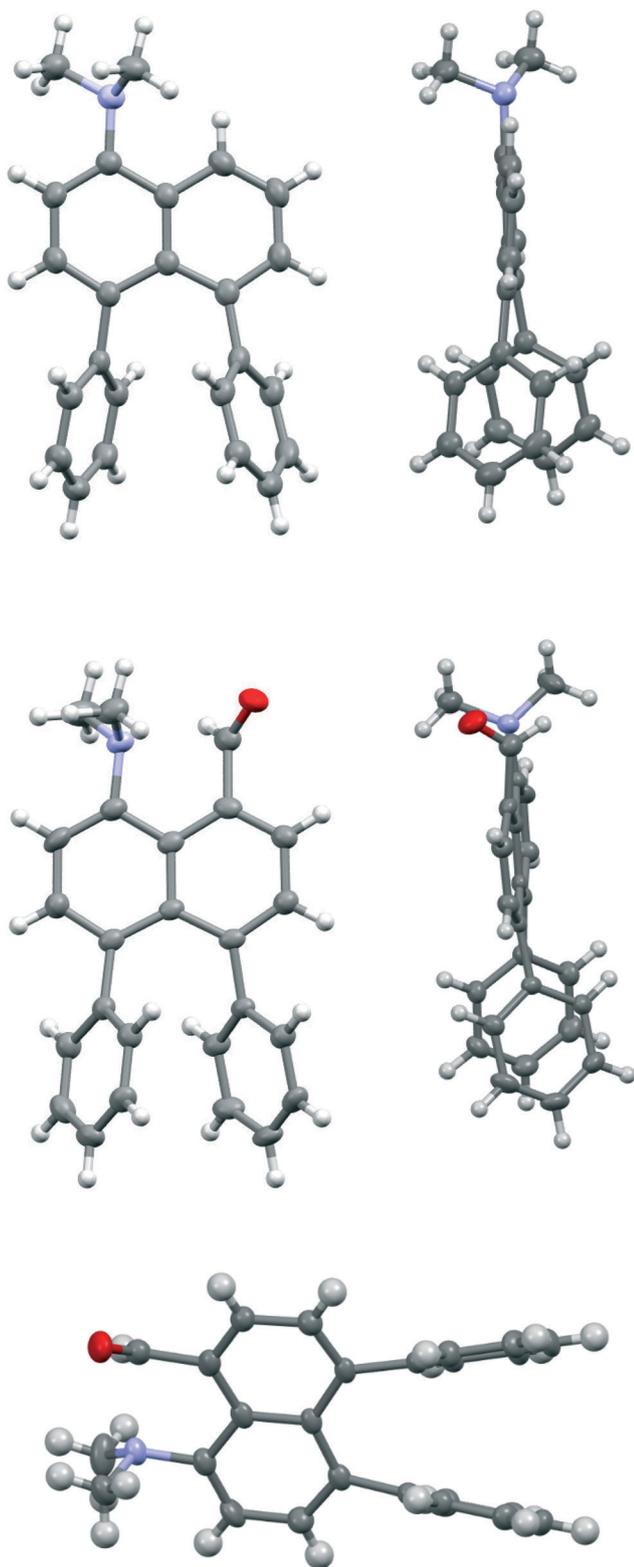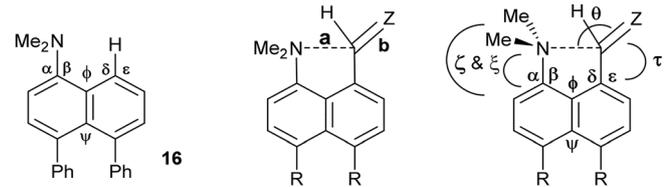
Fig. 1 Face-on and side-on views of the molecular structure of 1-dimethyamino-4,5-diphenylnaphthalene **16** (top), and of the corresponding *peri*-dimethyamino-aldehyde **17** (middle) showing the change in orientation of the dimethylamino group; side-on view of *peri*-aldehyde **17** (bottom) showing the splaying apart of the phenyl groups.

from the best naphthalene plane, and lie at 20.7° to each other (ESI:† Table S2). The phenyl groups are splayed apart in the naphthalene plane, with displacements of 4–4.5° from their symmetrical positions at their *peri*-attachment positions, and a contact of 3.012 Å between their *ipso* carbon atoms. The nearby *exo* angle ψ between the fused rings in the naphthalene core is expanded to 126.1(2)°. The latter leads to the corresponding *exo* angle ϕ at the naphthalene between the Me_2N and CHO groups being contracted to 117.5(2)° to produce a closer $Me_2N\cdots CHO$ separation of 2.309(3) Å. This is 0.18 Å shorter than in the case of **4**[4] without the two phenyl groups (2.489(6) Å). In other respects the molecular geometries of **17** and **4** are very similar (Table 1), for example the $Me_2N\cdots C{=}O$ angles are 112.56(17) and 113.5(3)° respectively. It is of note that the difference between the *exo* angles ϕ and ψ in the *peri*-amino-aldehyde **17** is larger than in the amine **16** which lacks an electrophilic *peri*-neighbour (8.6 v 5.4°) suggesting that the attractive Me_2N/CHO interaction contributes to this asymmetry in the *exo* angles.

We have already reported that a similar effect is shown in a crystal of the toluene solvate of the dinitrile **18**, where the installation of the two phenyl groups led to the reduction in the $Me_2N\cdots CH{=}C(CN)_2$ by 0.054 Å to 2.3603(19) Å[14] compared to the corresponding molecule **8**[8] without the phenyl substituents (Table 1). The phenyl groups take similar orientations to those in **16** and **17**, and the *exo* angles, ϕ and ψ, change to 117.74(12) and 126.24(13)° (Fig. 2). The larger separation between the two functional groups in dinitrile **18**, compared to the aldehyde **17** (2.359 *cf.* 2.309 Å) is mainly attributable to the larger displacements of the functional groups out of the naphthalene plane in opposite directions. It is important to note that the exact molecular structure is dependent on both the attraction between the groups and optimisation of crystal packing, thus for the *peri*-diphenyl series the $Me_2N\cdots C$ is shorter for the aldehyde than for the dinitrile (2.309 v 2.359 Å), but it is the other way round for the series without the phenyl groups (2.489 v 2.413 Å), though the differences are quite small.

Replacement of one of the nitriles in **18** with a methyl ester group has surprising consequences. Although, this compound has a similar open structure **20** in CDCl₃ solution according to NMR, in the crystal structure it adopts a closed zwitterionic structure **19** where the dimethylamino group has added to the alkene (Fig. 2), promoted by the presence of the diphenyl groups. In contrast, the analogue without the two phenyl groups, cyanoester **23**, adopts an open structure in the crystalline state with a $Me_2N\cdots CH{=}C(CN)CO_2Me$ separation of 2.595(2) Å, an even larger value than in the corresponding dinitrile **8** (Table 2).[8] The difference in *exo* angles for the closed structure is, of course, considerably larger than for the aldehyde **17** and dinitrile **18**: 17.6° v 8.6–8.9°. The formation of the five-membered ring reduces angle ϕ more and opens angle ψ further, illustrating the interdependence of these two angles. The disposition of the phenyl groups is similar to other diphenyl derivatives (Table S2†).

Table 1 Selected geometric details of *peri*-diphenylnaphthalene derivatives **16–18** and their corresponding analogues **4** and **8** without phenyl groups

17 Z = O, R = Ph
18 Z = C(CN)$_2$, R = Ph
4   Z = O, R = H
8   Z = C(CN)$_2$, R = H

	a/Å	b/Å	θ/°	ζ & ξ/°[a]	τ/°[a]	ΔN, C/Å[b]
16	—	—	—	23.9(2)/−105.1(2)	—	0.0646(19), —
17	2.309(3)	1.216(3)	112.56(17)	51.6(3)/−78.0(3)	58.9(3)	0.0610(19), −0.204(3)
18	2.3603(19)	1.356(2)	114.21(11)	36.9(2)/−94.95(18)	51.0(2)	0.2526(19), −0.4976(19)
4[4]	2.489(6)	1.213(6)	113.5(3)	44.5(5)/−85.2(5)	57.3(5)	0.220(3), −0.234(4)
8[8]	2.413(2)	1.354(2)	112.51(12)	49.7(2)/−81.5(2)	56.5(2)	0.166(2), −0.270(2)

	α/°	β/°	δ/°	ε/°	φ/ψ/°
Parent[c]	—	—	—	—	119.9(2)/126.2(2)
16	123.19(14)	117.65(14)	—	—	119.42(15)/124.78(14)
17	124.8(2)	114.8(2)	121.7(2)	118.1(2)	117.5(2)/126.1(2)
18	124.56(13)	115.34(12)	119.56(12)	119.83(12)	117.74(12)/126.24(13)
4[4]	124.3(4)	116.0(3)	122.2(4)	118.5(4)	120.6(3)/121.5(4)
8[8]	124.30(16)	115.92(14)	120.15(14)	120.27(14)	120.42(13)/122.65(15)

[a] ζ, ξ and τ: torsion angles. [b] ΔN, C: deviations of *peri* substituent atoms from the naphthalene's best plane. [c] Parent = 1,8-diphenylnaphthalene.[18]
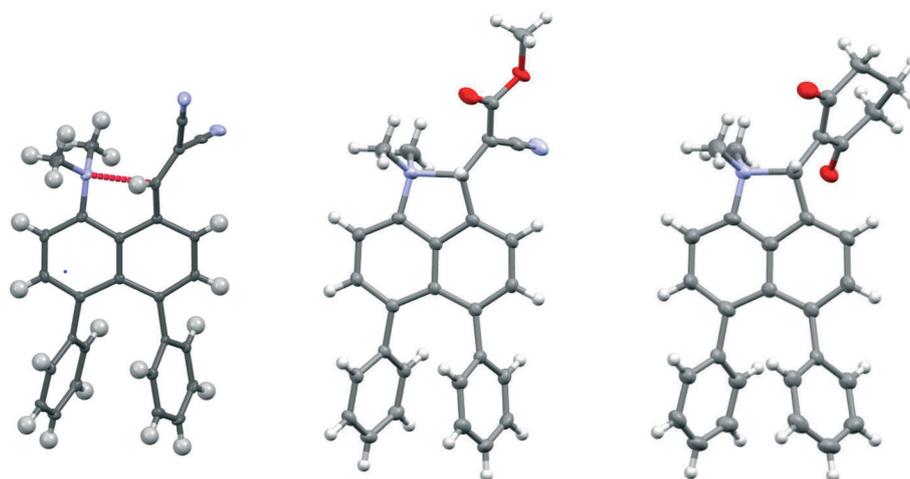
Fig. 2 Molecular structures of the *peri*-diphenyl naphthalene derivatives **18** (left), **19** (middle) and **21** (right).

The Me$_2$N–C bond formed between *peri*-substituents in **19** is 1.6719(14) Å long and the former alkene bond is now 1.4543(14) Å. In the two independent molecules of the biphenyl derivative **12**[13] where a dimethylamino group has added to an alkenedinitrile to form a less strained six-membered ring, the Me$_2$N–C bonds (1.586(3) and 1.604(3) Å) are more than 0.07 Å shorter than in **19**, and the broken alkene bonds (1.493(3) and 1.487(3) Å) are 0.04 Å longer than in **19**. Thus, in the naphthalene **19** the Me$_2$N–C bond can be considered as not fully formed, and the alkene bond as not fully broken. An earlier stage in the Michael reaction between the two groups is illustrated in the chloride salt of naphthalene **24** which has one *peri*-dimethylammonium group in place of the phenyl groups. In this case the Me$_2$N–C

bond is even longer (1.754(6) Å) than in **19**, and the former alkene slightly shorter (1.442(5) Å).[14]

23

24

25
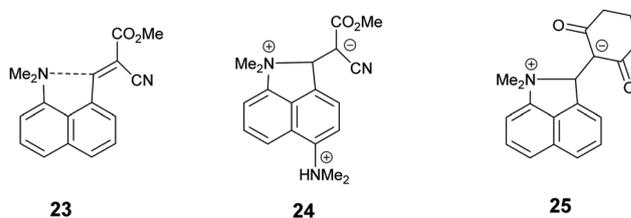
The accumulation of positive charge on the dimethylamino group in **19** leads to longer N–CH$_3$ bonds (1.4899(16) and 1.4932(15) Å *cf.* 1.4586(18) and 1.4639(17) in **23** without phenyl groups, and the development of negative charge on

Table 2 Selected geometric details for the ring-closed *peri*-diphenyl-naphthalene derivatives **19** and **21**, and the corresponding unsubstituted analogues **23** and **25**

19 X = CO₂Me, Y = CN; R = Ph

21 X,Y = (C(=O)CH₂)₂CH₂; R = Ph

25 X,Y = (C(=O)CH₂)₂CH₂; R = H

23
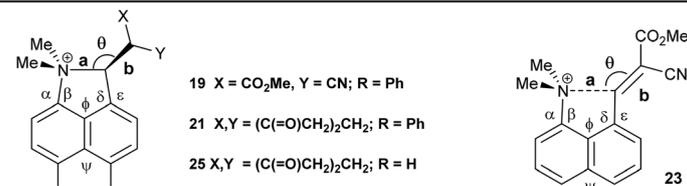
	a/Å	b/Å	θ/°	N–CH₃/Å	φ/ψ/°
19	1.6719(14)	1.4543(14)	115.94(9)	1.4899(16)/1.4932(15)	112.28(9)/129.88(9)
21	1.620(4)	1.484(4)	116.0(3)	1.503(4)/1.496(4)	111.6(3)/130.0(3)
23[14]	2.595(2)	1.3485(18)	116.23(10)	1.4586(18)/1.4639(17)	121.39(13)/122.56(12)
25[10]	1.6310(19)	1.4863(19)	113.99(10)	1.4995(17)/1.5020(18)	113.16(12)/128.31(14)

	α/°	β/°	δ/°	ε/°
19	127.80(9)	109.84(9)	110.75(9)	129.78(9)
21	126.7(3)	110.7(3)	110.3(3)	130.5(3)
23	123.15(13)	116.82(11)	122.53(12)	117.89(12)
25	128.64(12)	109.27(13)	109.46(12)	131.62(14)

the carbon atom between the nitrile and ester groups causes the bonds from the carbanionic centre to these groups to be shortened (C–CN, C–C(=O): 1.4100(15) and 1.4289(14) Å *cf.* 1.4420(18) and 1.4851(19) Å in **23**). Furthermore, the lengths of both bonds from the naphthalene ring to the *peri*-groups are increased on the formation of the bond between them: (C(nap)–N, C(nap)–C: 1.4720(12), 1.5058(14) Å *cf.* 1.4259(17) and 1.4772(19) Å in **23**).

Study of a crystal of the chloroform solvate of **21**, the Knoevenagel product formed from the diphenyl aldehyde **17** with cyclohexan-1,3-dione, showed that it also adopts a closed structure, as does its analogue without *peri*-phenyl groups **25**.[10] The Me₂N–C bond (1.620(4) Å) is 0.05 Å shorter than in the corresponding cyanoester **19** and the bond to the carbanion centre (1.484(4) Å) is 0.03 Å longer due to the stronger carbanion

stabilising ability of two ketone groups compared to an ester and a nitrile group. The presence of the two phenyls has made little difference to the Me₂N–C bond compared to that the analogue **25** without phenyl groups. The expected small increase and decrease in the *exo* angles ψ and ϕ respectively, are compensated by changes in the angles at the *peri*-substituents (α, β, δ and ε). It is of note that for the diphenylnaphthalene derivatives whose crystals do not include solvent, **16**, **17**, and **19**, there is common packing motif, in which two molecules lie such that the two phenyl groups of one lie over the naphthalene of the other and *vice-versa* (Fig. S1, ESI†).

Addition of acid to the aldehyde **17** leads to protonation of the carbonyl group and formation of a N–C bond between the *peri*-groups. Thus, addition of HCl gave the chloride salt **26** as a DCM solvate, while an attempted Knoevenagel reaction with Meldrum's acid gave the analogous salt with a monomalonate anion **27** (Scheme 2). The crystal structures of both salts were determined (Fig. 3, Table 3). The phenyl groups have enhanced the difference in the *exo* angles ψ and φ between the *peri*-positions from 14.4° in naphthalene salt **5**[5] which has no *peri*-phenyl groups, to 18.2–18.4° in cations **26** and **27**. This leads to shorter Me₂N–C(OH) bonds, 1.617(5) and 1.621(2) Å, compared to **5** (1.638(2) Å) without the phenyl groups, and correspondingly the C–OH bonds are slightly longer: 1.360(4) and 1.363(2) v 1.353(2) Å. The anion in each
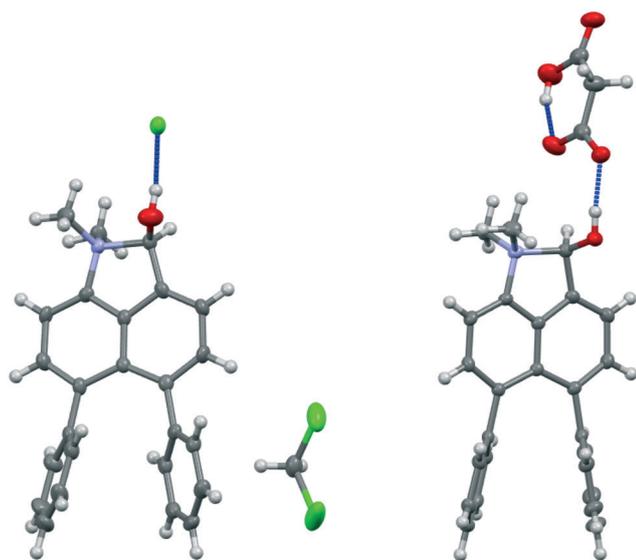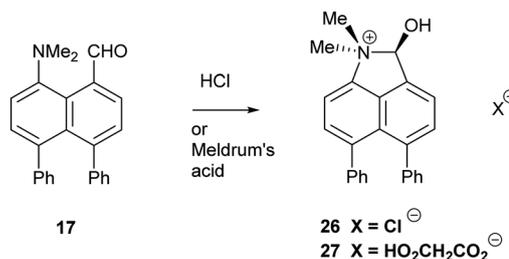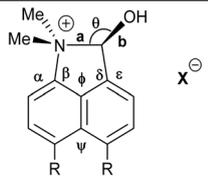

Fig. 3 Salts formed from aldehyde **17** by O-protonation: a chloride salt **26** as a DCM solvate (left) and a monomalonate salt **27** (right).

Scheme 2 Preparation of salts of **17**.

26 X = Cl⁻

27 X = HO₂CH₂CO₂⁻

Table 3 Selected geometric details of cations in salts **26**, **27** and **5**

26. R = Ph; X = Cl
27. R = Ph; X = monomalonate
5. R = H; X = Cl

	a/Å	b/Å	N–CH$_3$/Å	θ/°	φ/ψ/°
26	1.617(5)	1.360(4)	1.491(5)/1.499(5)	111.3(3)	112.1(3)/130.3(4)
27	1.621(2)	1.363(2)	1.487(3)/1.499(2)	110.92(15)	112.03(17)/130.42(17)
5[5]	1.638(2)	1.353(2)	1.497(2)/1.498(2)	111.64(12)	113.92(15)/128.32(15)

salts form a hydrogen bond to the cation's hydroxyl group (Fig. 3). All these structures with two *peri*-phenyl groups show evidence of the effect of the repulsion between the two phenyl groups on shortening the interaction or bond between the two opposite *peri*-groups, and in the case of **19** forcing the formation of the bond in the solid state.

Attempted reaction of aldehyde **17** with nitromethane in the presence of ethylenediammonium diacetate led to a small amount of the crystalline *bis*-imine **22**, formed by reaction between two equivalents of the aldehyde **17** and one of the catalyst, whose structure was determined by X-ray crystallography (Fig. 4). The structure is particularly informative with respect to the influence of the *peri*-phenyl groups. The imine and Me$_2$N- groups are not well oriented for mutual interaction, both preferring to conjugate with the naphthalene ring. The two imine bonds make torsions of 36.4(3) and 42.0(3)° to their nearest aromatic C,C(H) bonds, and for both of the pyramidal –NMe$_2$ groups one N-methyl bond make a torsion angle of just 23.1(3) and 26.0(3)° to the nearest aromatic C,C(H) bond.

The Me$_2$N···C separations are quite long (2.667(3) and 2.711(3) Å) and their angles of interaction (Me$_2$)N···C=N are not favourable (125.84(15) and 129.12(15)°). In contrast to the other structures discussed above, the phenyl groups have a much lower distorting effect on the two *exo* angles at either side of each naphthalenes. Thus, instead of a difference of 8.5/8.6° between *exo* angles ψ and φ seen in **17** and **18**, this is reduced to 1.8 and 2.6° in the two naphthalenes of the *bis*-imine. However, the naphthalene rings are strongly twisted, with angles of 9.9 and 11.5° between their benzene rings' best planes, so that all four sets of *peri*-substituent atoms are strongly displaced out of their best naphthalene planes, to opposite sides, by 0.271(2)–0.605(2) Å. The relative dispositions of the phenyl groups relative to the naphthalene plane and at the *peri*-positions, however, remain similar to those in the other diphenyl derivatives (Table S1†). In the case of *bis*-imine **22** the phenyl groups do not exert their normal effect because the Me$_2$N/C=NR interactions are not attractive enough, or possibly repulsive, at *ca.* 2.5 Å.[19] In this case, faced with two unfavourable *peri* interactions, the
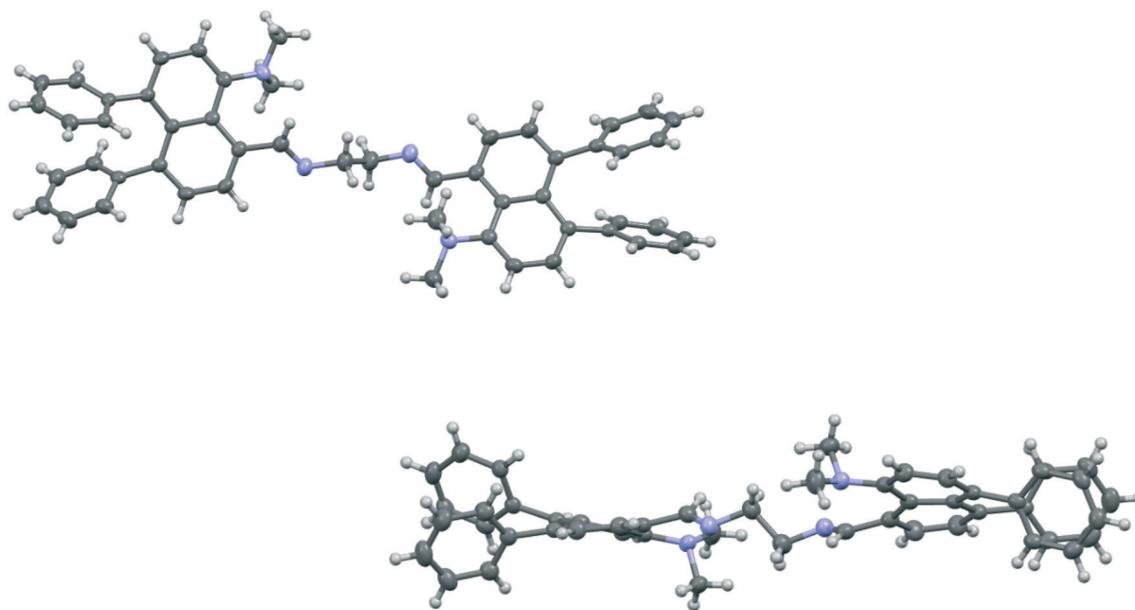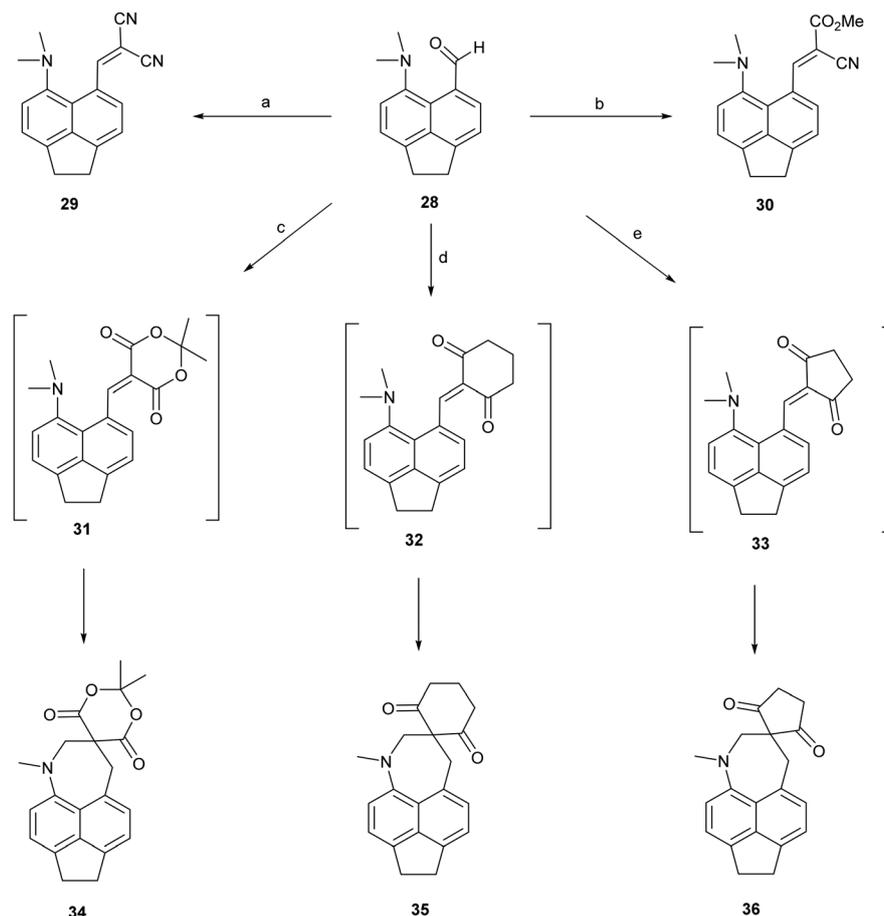

Fig. 4 Face-on view of *bis*-imine **22** (top) and a view through one naphthalene ring's plane showing the strong displacement of all pairs of *peri*-substituents out of their naphthalene planes (bottom).

Scheme 3 (a) and (b): Malononitrile or methyl cyanoacetate/ethylenediammonium diacetate cat./methanol/reflux; (c)–(e) Meldrum's acid, cyclohexane-1,3-dione or cyclopentane-1,3-dione, DMSO, RT.

naphthalene rings distort strongly out of the aromatic plane, rather than within it, and so move the *peri*-substituents apart. Thus, there are limits to the compressive influence of the two *peri*-phenyl groups on an opposite set of *peri*-substituents.

Acenaphthene derivatives

To test the effect of tightening the opposite *exo* angle ψ on the separation of the interacting functional groups a series of acenaphthene derivatives which have an ethylene bridge between the second set of *peri*-positions was synthesized (Scheme 3). Aldehyde **28** was prepared from the known *peri*-dimethylamino-bromoacenaphthene[16] by halogen-lithium exchange and treatment with DMF in 55% yield. Knoevenagel condensations of aldehyde **28** with malononitrile and methyl cyanoacetate, catalysed by ethylenediamine diacetate in refluxing methanol yielded **29**[14] and **30** in 88–91% yields. However, reaction with cyclic dicarbonyl compounds: Meldrum's acid, cyclohexane-1,3-dione and cyclopentane-1,3-dione in DMSO at room temperature with no catalyst, gave directly the fused azepines **34–36**, formed by reaction between the functional groups of the initially formed Knoevenagel products **31–33**. The structures of **28–30** and

34–36 were determined by X-ray crystallography. For **28–30** the small *exo* angle ψ within the five membered ring of the acenaphthene (111.25(18)–111.73(17)°) leads to a larger *exo* angle ϕ between the two functional groups (127.03(18)–129.50(14)°), which increases the distance between them, the opposite to what was observed for the diphenyl derivatives. In the same way, it is the added space between the functional groups in the expected Knoevenagel products **31–33** which leads to a ready reaction between them which is initiated by hydride transfer from the N–CH$_3$ group to the polarised alkene according to the tertiary amino effect.[20,21]

The structure of the aldehyde **28** shows a very significant difference to that of the corresponding naphthalene derivative **4** without the ethylene bridge (Fig. 5, Table 4). The two groups are splayed apart to a Me$_2$N···C separation of 2.953(2) Å, *cf.* 2.489(6) Å in **4**, due mainly to a widening of the ϕ *exo* angle to 129.50(14)°, and the aldehyde group has rotated so that it now it lies at just 16.4° to the nearest C, C(H) bond of the aromatic system. Thus, it is not involved in a n–π* interaction of type: Me$_2$N···C=O as it is in **4**. The nitrogen atom lies at 2.37 Å from the aldehyde hydrogen atom, and its theoretical lone pair axis lies at 27° to the N···H vector. Both the aldehyde and dimethylamino groups
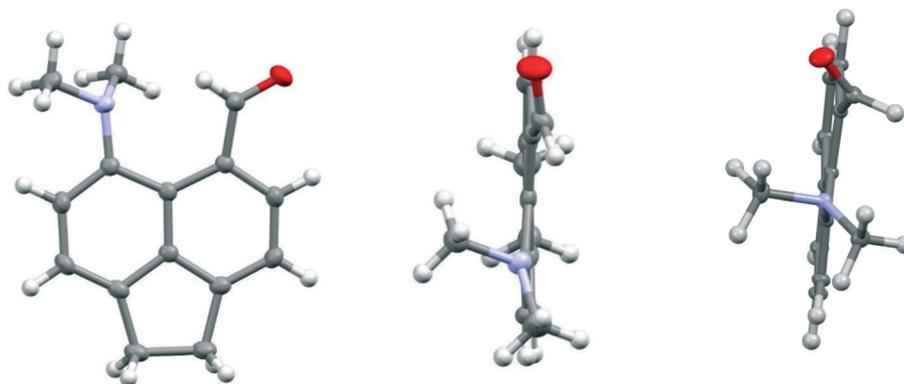
Fig. 5 Two views of the acenaphthene aldehyde **28** (left and middle), showing how the aldehyde group lies close to the aromatic plane and the pyramidal dimethylamino group is oriented to conjugate with the aromatic ring, in contrast to the corresponding naphthalene without an ethylene bridge **4** (right).[4]

Table 4 Selected geometric details for the acenaphthenes **28**–**30**

28: X = O

29: X = C(CN)$_2$

30 X = C(CN)(CO$_2$Me)

	a/Å	b/Å	θ/°	ζ, ξ/°[a]	τ/°[a]
28	2.953(2)	1.2167(18)	149.68(11)	18.8(2)/−111.32(16)	17.4(2)
29	2.846(2)	1.348(3)	133.00(15)	27.5(3)/−100.8(2)	35.9(3)
	2.755(2)	1.343(3)	122.71(14)	45.8(3)/−82.1(2)	51.9(3)
30	2.843(2)	1.340(2)	129.28(11)	27.5(2)/−99.97(18)	40.8(2)

	α/°	β/°	δ/°	ε/°	ϕ/ψ/°
28	121.74(13)	119.27(13)	124.14(13)	116.08(13)	129.50(14)/111.38(13)
29	121.81(18)	119.57(17)	121.32(18)	119.88(18)	128.54(17)/111.25(18)
	122.77(18)	118.23(16)	121.87(12)	119.47(17)	127.30(18)/111.73(17)
30	121.76(13)	119.53(12)	121.36(12)	119.72(12)	128.62(13)/111.47(13)

[a] ζ, ξ and τ: torsion angles.
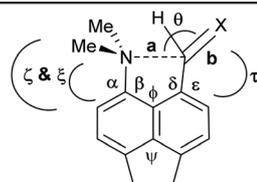
are oriented to optimise their conjugation with the acenaphthene ring, though the bond lengths between these groups and the ring are not significantly shortened compared to **4**: Me$_2$N–C: 1.4221(19) v 1.420(6) Å, and (O═)C–C: 1.480(2) v 1.490(6) Å for **28** and **4** respectively. The dimethylamino group is displaced slightly towards the aldehyde, and the aldehyde is displaced more strongly away, but it is the larger *exo* angle which is the main cause of their increased separation.

The structures of the Knoevenagel products **29** and **30** have a similar pattern of in-plane displacements as in the aldehyde **28** due to the widening of the ϕ *exo* angle to 127.03(18)–128.62(13)/Å, but the alkenes lie at greater angles (35.9(3)–51.9(3)°) to their acenaphthene rings (Fig. 6, Table 4). The Me$_2$N⋯C separations lie in the range 2.755(3)–2.846(3) Å with the shortest for one of two crystallographically independent molecule of dinitrile **29** which has the largest rotation of the alkene group away from the acenaphthene. In this case the Me$_2$N⋯C═C angle is reduced to 122.68(14)° (*cf.*

129.28(11) and 133.00(15)° in the other cases), and this can be considered as a rather long n–π* interaction.
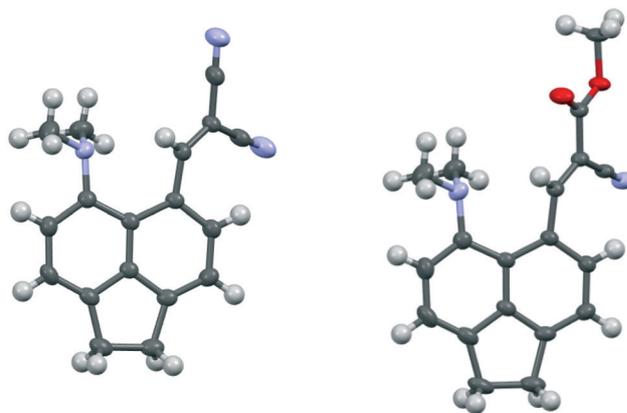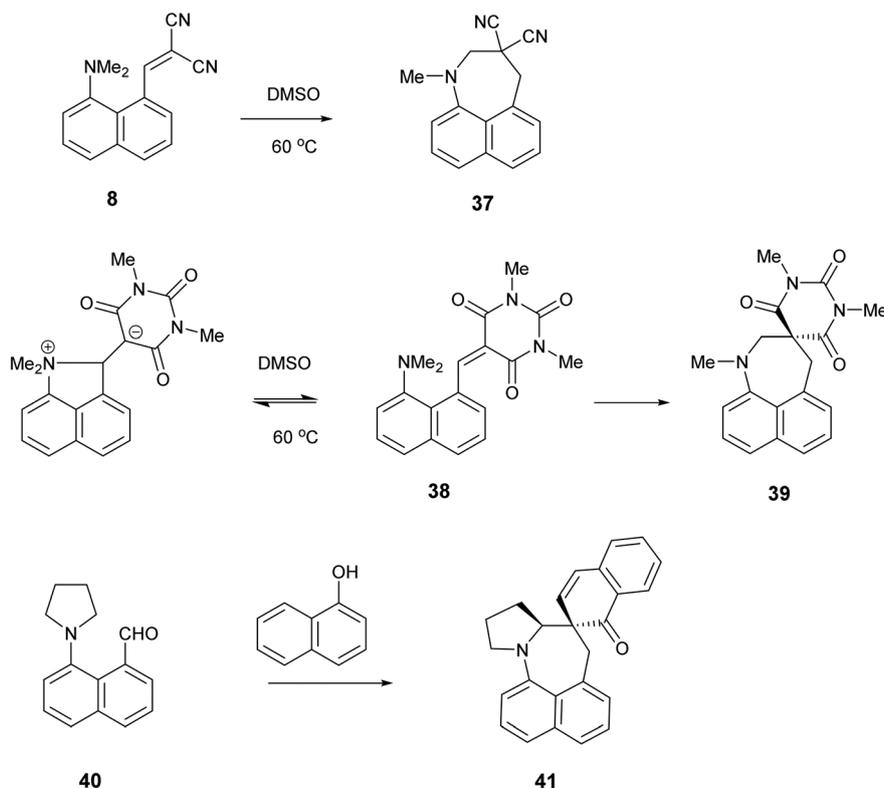

Fig. 6 Molecular structures of one of the two molecules of dinitrile **29**, with the larger rotation of the dinitrile side chain, (left) and of cyanoester **30** (right).

Scheme 4 Examples of the conversion of *peri*-aminonaphthalene systems **8**, **38** and **40**[22–24] to *spiro* derivatives initiated by the tertiary amino effect.

It is known that for a naphthalene with a *peri*-dimethylamino group located next to an electron deficient alkene, on heating in DMSO at 60° C the groups react to form a fused azepine, for example from the dinitrile **8** or the *N,N*-dimethylbarbiturate derivative **38** to the fused azepines **37** and **39** (Scheme 4).[22,23] Furthermore, recent related work has reported how 2-naphthol reacts with the *peri*-pyrrolidinyl aldehyde **40** to give **41**.[24] These reactions are triggered by the tertiary amino effect[20,21] whereby a hydride from the N–CH$_2$ or N–CH$_3$ group adds to the polarised alkene, and then the iminium cation and the carbanion formed add to each other (Scheme 5). In the case of the attempted preparation of the acenaphthene Knoevenagel products **31–33**, the reaction goes directly to the azepine by stirring aldehyde with the

dicarbonyl compound in DMSO at room temperature in 40 to 80% yields. The widening of the *exo* angle allows the groups to get into positions to react more easily. The structures of the resulting three fused azepines **34–36** with various spiro cyclic dicarbonyl systems are shown in Fig. 7, with selected geometric data in Tables S4 and S5 (ESI†).

The structures are similar to related naphthalene based systems[10] except that the widening of the ϕ angle is retained. The N–C(H$_2$)–C(spiro) ring atoms are displaced to the same side of the acenaphthene ring, with the strongest displacements for the methylene and *spiro* carbons (1.163–1.354 and 0.551–0.919 Å respectively). The remaining methylene carbon is displaced to a smaller degree in the opposite sense (Table S5†). Within the azepine ring, the nitrogen atom adopts partial pyramidal
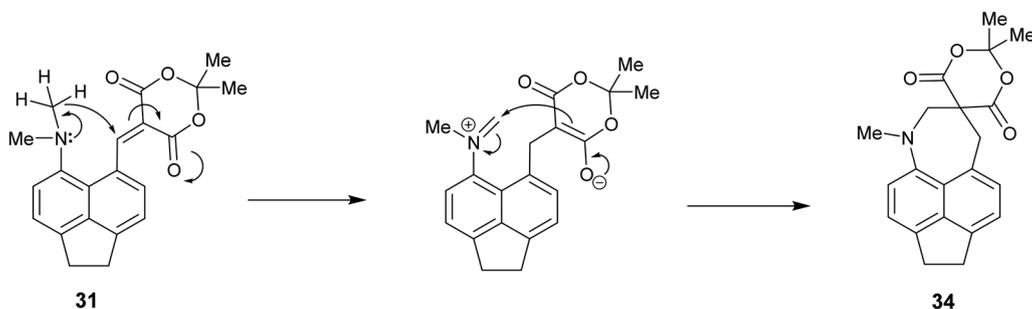
Scheme 5 Mechanism of formation of *spiro* system **34** from Knoevenagel product **31** initiated by hydride transfer from the *N*-methyl group to the activated alkene.
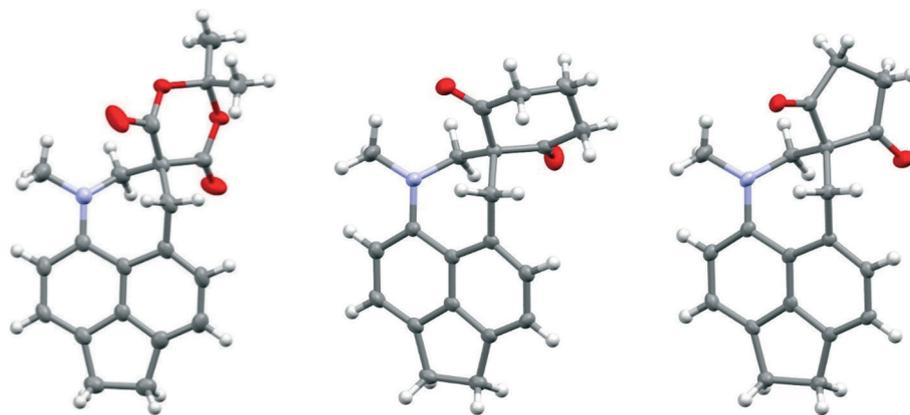
Fig. 7 Molecular structures of the *spiro* acenaphtho-azepines **34**, **35** and **36** (left to right).

bonding geometry (sum of angles: 343.6–349.6°), one bond to the *spiro* centre is strained (1.551–1.562 Å), and the angles at nitrogen and the methylene carbons show notable angle strain (113–117°). These are the first reported *spiro* derivatives of this fused azepine system.

Fluorene derivatives

To provide a skeleton to contrast with the biphenyl system but with the phenyl rings constrained to be near coplanar and with the separation between *ortho* substituents increased, the 9,9-dimethyl-fluorene skeleton **42** was selected. The parent dimethyl-hydrocarbon was converted to the *ortho*-diiodo compound **43** by *bis*-lithiation and treatment with iodine in 25% yield. The structure of the diiodo compound was confirmed by X-ray crystallography, and it shows considerably distortion of the fluorene system to accommodate an intramolecular I⋯I contact distance of 3.6392(4) Å (further details in the ESI†). *Mono*-Lithiation of diiodo compound **43** and treatment with DMF gave the dimethylamino aldehyde **44** in one step in 42% yield. The

reaction proceeds by addition of DMF to the *mono*-lithiated aromatic, followed by expulsion of dimethylamide which substitutes the adjacent iodide. Barbasiewicz *et al.* has observed a similar reaction with *peri*-diiodonaphthalene.[25]

The aldehyde **44** gave the expected alkenes **45** and **46** by Knoevenagel reaction with malononitrile or nitromethane under reflux in methanol with ethylenediammonium diacetate as catalyst (Scheme 6). In contrast, just stirring aldehyde **44** with benzoyl-nitromethane, Meldrum's acid or cyclopentane-1,3-dione in DMSO at 20 °C gave fused azocine products **47–49**, analogous to the behaviour of the more reactive acenaphthene derivatives (Scheme 7). Interestingly, on recrystallisation, some of the *gem*-benzoyl-nitro derivative **49** lost the benzoyl group, presumably due to the effect of water in the solvent, to give the fused nitro-azocine **50** (Scheme 7). Similar types of azocines have been reported from disubstituted biphenyls,[21] however, we are not aware of any such derivatives of the fluoreno-azocine ring system in **47–50**. The crystal structures of **44** and **45** were determined to examine the interaction between functional groups, and of **48** and **50** to confirm their molecular structures.
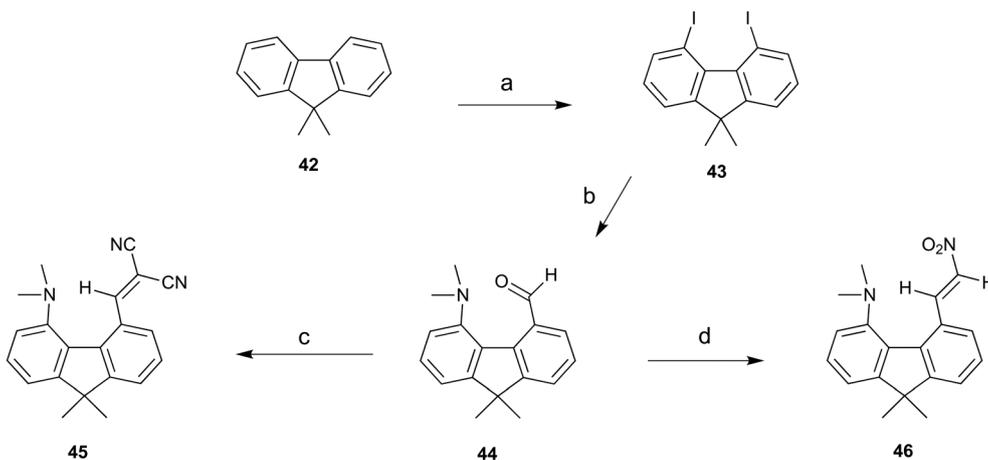
Scheme 6 a) *n*-BuLi/TMEDA/60 °C/5 h, then I₂/THF −78 °C; b) *n*-BuLi/ether/−78 °C then DMF, warm to 20 °C; (c) and (d) malononitrile or nitromethane/ethylenediammonium diacetate cat./methanol/reflux.
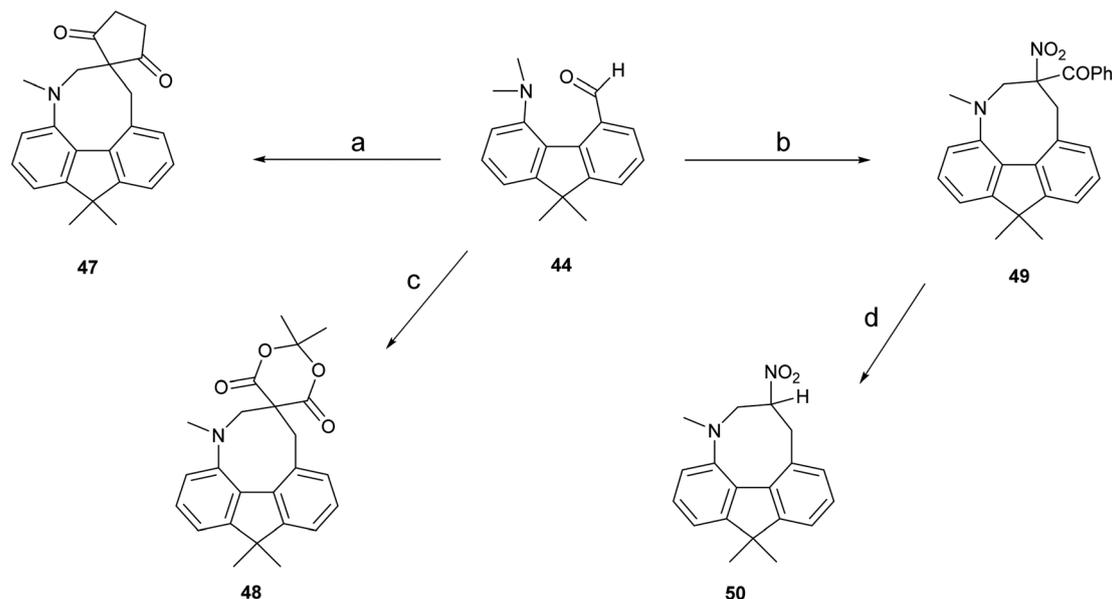
Scheme 7 (a)–(c): Cyclopentane-1,3-dione, PhCOCH$_2$NO$_2$, or Meldrum's acid/DMSO/20 °C; (d): heat in DCM/hexane in air.
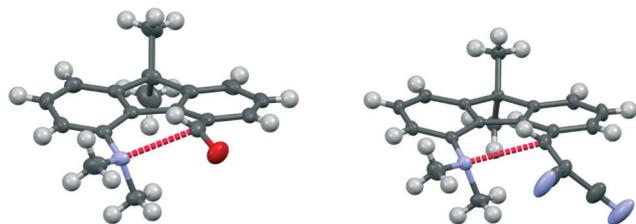

Fig. 8 Molecular structures of fluorenes **44** (left) and **45** (right), with the long n–π* interaction shown in red.

The aldehyde and ethenedinitrile derivatives **44** and **45** adopt similar molecular conformations, with Me$_2$N···C separations of 2.691(3) and 2.8304(17) Å (Fig. 8, Table 5). In contrast, in the biphenyl series, the corresponding separations are quite different: 2.989(2) and 1.586(3)/1.604(3) Å respectively. In **44** the lack of rotational freedom in the

fluorene has brought the Me$_2$N- and –CHO functional groups closer together, and the Me$_2$N···C=O angle is 111.04(16)°, as would be expected for a n–π* interaction. The axis of the nitrogen lone pair lies at 9.5° to the Me$_2$N···C(=O) vector. The greater separation of Me$_2$N- and –CH=C(CN)$_2$ groups in the constrained fluorene system **45**, prevents the bond formation seen in the biphenyl series. The Me$_2$N···C=C angle is favourable for n–π* interaction (110.80(10)°), though the Me$_2$N···C distance is particularly long 2.8304(17) Å and the angle between the axis of the N lone pair and the Me$_2$-N···C vector is 8.5°. In the fluorene plane the Me$_2$N- group is displaced towards the alkene which is displaced away, but the favourable alignment of groups in **44** and **45** are achieved by different combinations of (a) displacements of the groups to the opposite sides of the fluorene plane and (b) widening of the *exo* angles at the intervening ring fusions (Table 5).

Table 5 Selected molecular geometry data for fluorene derivatives **44** and **45**

44 X = O

45 X = C(CN)$_2$

	a/Å	θ/°	ζ & ξ/°[a]	τ[a]/°	ΔN, C[b]	
44	2.691(3)	111.04(16)	25.4(3)/−105.6(2)	40.6(3)	0.496(2), −0.578(3)	
45	2.8304(17)	110.80(10)	15.84(18)/−111.65(14)	42.5(2)	0.5588(15), −0.3079(15)	

	α/°	β/°	γ/°	γ'/°	δ/°	ε/°
44	123.52(18)	118.93(18)	130.90(18)	131.8(2)	124.25(19)	117.46(19)
45	122.20(11)	120.13(11)	133.71(12)	133.51(11)	122.75(11)	118.92(12)

[a] ζ, ξ and τ: torsion angles. [b] ΔN, C: deviations of the 1- and 8- substituent atoms from the fluorene plane.
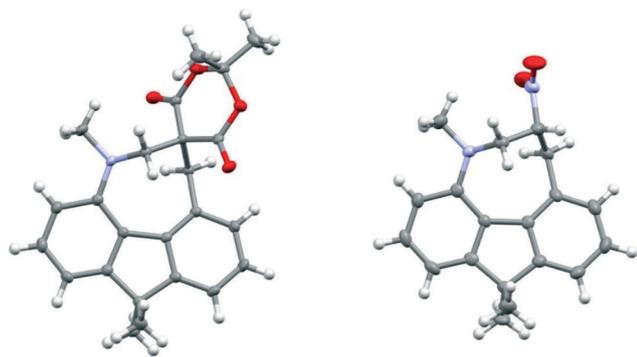
Fig. 9 Molecular structures of fused azocines **48** (left) and **50** (right).

X-ray crystallography also confirmed the structures of two of the fused azocines, **48** and **50** which are shown in Fig. 9 with selected molecular geometry in Tables S6 and S7 (ESI†). The *spiro* junction in the azocine ring of **48** leads to more sp^3C–sp^3C bond strain with C–C bonds of 1.561(2) and 1.565(2) Å to the *spiro* atom, than in the nitro derivative **50** (1.506(4) and 1.525(4) Å). In the azocine ring the nitrogen atom adopts a moderately pyramidal bonding geometry (sum of angles: **48**: 350.60(13)°; **50**: 348.8(2)°), and there is significant angular strain along the N–CH₂–C–CH₂ fragment (112.0–118.26°) with exception of the *spiro* carbon of **48**. The N–C(H₂)–C ring atoms are displaced to the same side of the fluorene ring, with the strongest displacements for the two carbons (1.430–1.458 and 0.847–0.953 Å). The remaining methylene carbon is displaced to a smaller degree in the opposite sense (Table S7†). These out of plane displacements are larger than in the related acenaphthene derivatives.

Conclusions

These investigations show that the interaction between an electrophile and a nucleophile in the *peri*-positions of a naphthalene can be modified by the choice of substituents at the opposite *peri*-positions. Two phenyl groups repel each other and force the other substituents closer, and in one case, the cyanoester derivative **19**, led to them forming a bond, which in the absence of the phenyls they did not. In contrast, in acenaphthene systems, the ethylene group, acts as a short constraint between the *peri*-positions, widening the separation between the interacting groups, with various consequences. The aldehyde group in compound **28** now has sufficient space to rotate into the plane of the aromatic system so the n–π* interaction is lost, while for the ethenedinitrile in **29** the Me₂N···C interaction in lengthened, and for more reactive electrophiles cyclisation between the *N*-methyl group and the alkene occurs forming a fused azepine ring as in **34–36**, initiated by intramolecular hydride transfer, which the increased space between groups permits. For the 1,6 interactions in the fluorene derivatives studied, two long n–π* interactions were observed for the less reactive electrophiles in **45** and **46**, but for the more reactive the

corresponding cyclisation to form fused azocine rings in **48** and **50** took place. The *peri*-diphenylnaphthalene system is the most promising for exploring further nucleophile–electrophile interactions and, in particular, at accessing those separations nearer to the transition state for the direct bond formation. Additions of small groups to the phenyl rings to increase the repulsion between them may lead to even closer *peri*-interactions at the opposite positions, and complement the very few N···C interactions known in the 1.7–2.3 Å range.[14] In this work we did not find, but also did not deliberately look for, polymorphs of the compounds whose crystal structures were determined. It is possible that different polymorphs or solvates may show somewhat different interactions between the groups, as a result of the effects of the different packing arrangements, just as in the crystal structure of the acenaphthene **29** the two independent molecules have differences in their conformations. In the diphenylnaphthalene series, in particular, this may be worth pursuing.

Experimental

Conflicts of interest

There are no conflicts of interest to report.

Acknowledgements

References

1 *Structure Correlation*, ed. H.-B. Bürgi and J. D. Dunitz, VCH, Weinheim, 1994, vol. 1.

2 H.-B. Bürgi, J. D. Dunitz and E. Schefter, *J. Am. Chem. Soc.*, 1973, **95**, 5065–5067.

3 W. B. Schweizer, G. Procter, M. Kaftory and J. D. Dunitz, *Helv. Chim. Acta*, 1978, **61**, 2783–2808.

4 D. R. W. Hodgson, A. J. Kirby and N. Feeder, *J. Chem. Soc., Perkin Trans. 1*, 1999, 949–954.

5 A. Wannebroucq, A. P. Jarmyn, M. B. Pitak, S. J. Coles and J. D. Wallis, *Pure Appl. Chem.*, 2016, **88**, 317–331.

6 P. C. Bell, W. Skranc, X. Formosa, J. O'Leary and J. D. Wallis, *J. Chem. Soc., Perkin Trans. 2*, 2002, 878–886.

7 M. Parvez and I. I. Schuster, *Acta Crystallogr., Sect. C: Cryst. Struct. Commun.*, 1990, **46**, 947–948.

8 P. C. Bell and J. D. Wallis, *Chem. Commun.*, 1999, 257–258.

9   J. O'Leary, W. Skranc, X. Formosa and J. D. Wallis, *Org. Biomol. Chem.*, 2005, **3**, 3273–3283.

10 A. Lari, M. B. Pitak, S. J. Coles, G. J. Rees, S. P. Day, M. E. Smith, J. V. Hanna and J. D. Wallis, *Org. Biomol. Chem.*, 2012, **10**, 7763–7779.

11 A. F. Pozharskii, O. V. Dyablo, O. G. Pogosova, V. A. Ozeryanskii, A. Filarowski, K. M. Vasilikhina and N. A. Dzhangiryan, *J. Org. Chem.*, 2020, **85**, 12468–12481; C. Cox, H. Wack and T. Lectka, *Angew. Chem., Int. Ed.*, 1999, **38**, 798–800.

12 M. W. Stanford, F. R. Knight, K. S. Athukorala Arachchige, P. Sanz Camacho, S. E. Ashbrook, M. Bühl, A. M. Z. Slawin and J. D. Woollins, *Dalton Trans.*, 2014, **43**, 6548–6560; F. R. Knight, R. A. M. Randall, K. S. Athukorala Arachchige, L. Wakefield, J. M. Griffin, S. E. Ashbrook, M. Bühl, A. M. Z. Slawin and J. D. Woollins, *Inorg. Chem.*, 2012, **51**, 11087–11097.

13 J. O'Leary and J. D. Wallis, *Org. Biomol. Chem.*, 2009, **7**, 225–228.

14 J. C. Bristow, I. Naftalin, S. V. A. Cliff, S. Yang, M. Carravetta, R. Stern, I. Heinmaa and J. D. Wallis, *CrystEngComm*, 2020, **22**, 6783–6795.

15 E. Hupf, N. Olaru, C. I. Rat, M. Fugel, C. B. Hübschle, E. Lork, S. Grabowsky, S. Mebs and J. Beckmann, *Chem. – Eur. J.*, 2017, **23**, 10568–10579.

16 D. Pla, O. Sadek, S. Cadet, B. Mestre-Voegtlé and E. Gras, *Dalton Trans.*, 2015, **44**, 18340–18346.

17 C. F. R. A. C. Lima, J. E. Rodriguez-Borges and L. M. N. B. F. Santos, *Tetrahedron*, 2011, **67**, 689–697.

18 K. Komatsu, K. Taekuchi, M. Shiro, S. Cohen and M. Rabinovitz, *J. Phys. Org. Chem.*, 1993, **6**, 435–444.

19 N. Asaad, J. E. Davies, D. R. W. Hodgson, A. J. Kirby, L. van Vliet and L. Ottavi, *J. Phys. Org. Chem.*, 2005, **18**, 101–109.

20 L. Wang and J. Xiao, *Top. Curr. Chem.*, 2016, 17; O. Meth-Cohen and H. Suschitsky, *Adv. Heterocycl. Chem.*, 1972, **14**, 211–278.

21 Á. Polonka-Bálint, C. Saraceno, K. Ludányi, A. C. Bényei and P. Mátyus, *Synlett*, 2008, 2846–2850.

22 Á. A. Földi, K. Ludányi, A. C. Bényei and P. Mátyus, *Synlett*, 2010, 2109–2113.

23 A. F. Pozharskii, M. A. Povalyakhina, A. V. Degtyarev, O. V. Ryabtsova, V. A. Ozeryanskii, O. V. Dyablo, A. V. Tkachuk, O. N. Kazheva, A. N. Chekhlov and O. A. Dyachenko, *Org. Biomol. Chem.*, 2011, **9**, 1887–1900.

24 S. S. Li, X. Lv, D. Ren, C.-L. Shao, Q. Liu and J. Xiao, *Chem. Sci.*, 2018, **9**, 8253–8259.

25 K. Grudzień, K. Żukowska, M. Malińska, K. Woźniak and M. Barbasiewicz, *Chem. – Eur. J.*, 2014, **20**, 2819–2828.